Supplement of

U-Surf: A Global 1km spatially continuous urban surface property dataset for kilometer-scale urban-resolving Earth system modeling

Yifan Cheng et al.

**Correspondence to*:
Lei Zhao (leizhao@illinois.edu), TC Chakraborty (tirthankar.chakraborty@pnnl.gov), and Weilin Liao (liaoweilin@mail.sysu.edu.cn)

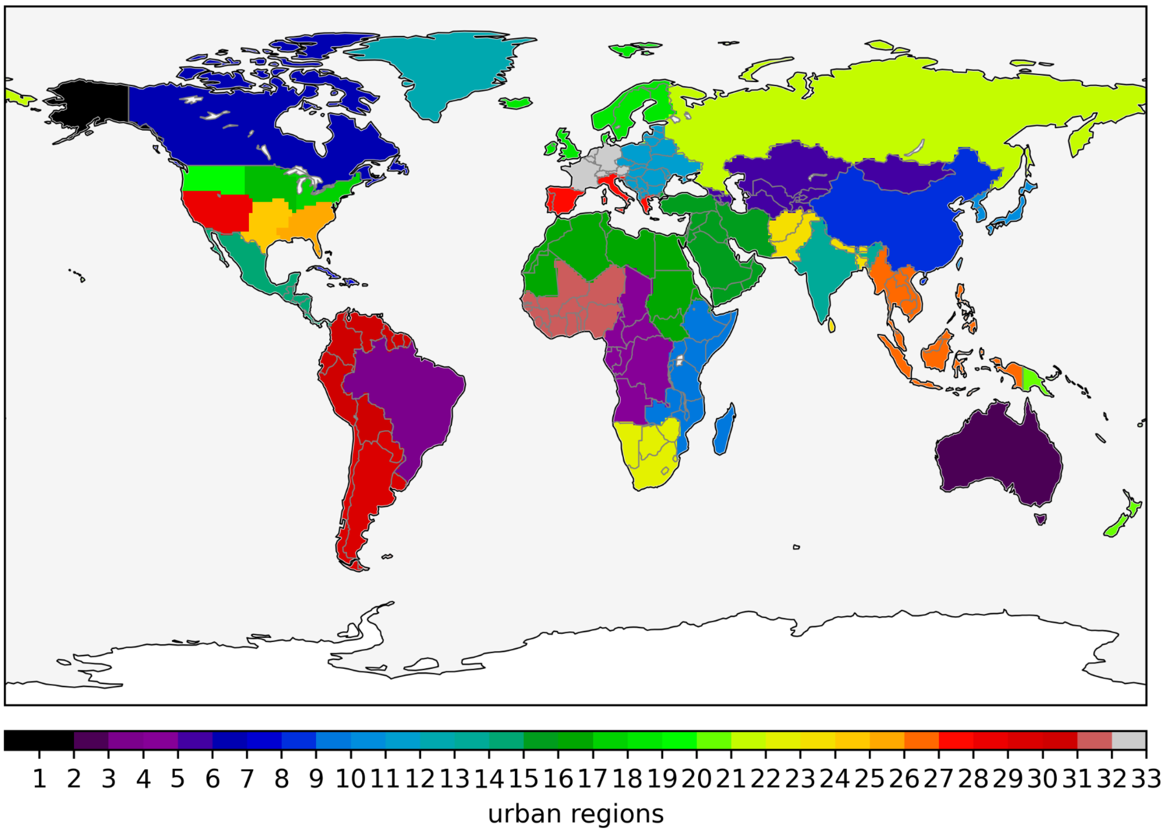

Figure S1. The thirty-three regions used to constrain the global variability of urban surface properties in Jackson et al., (2010).

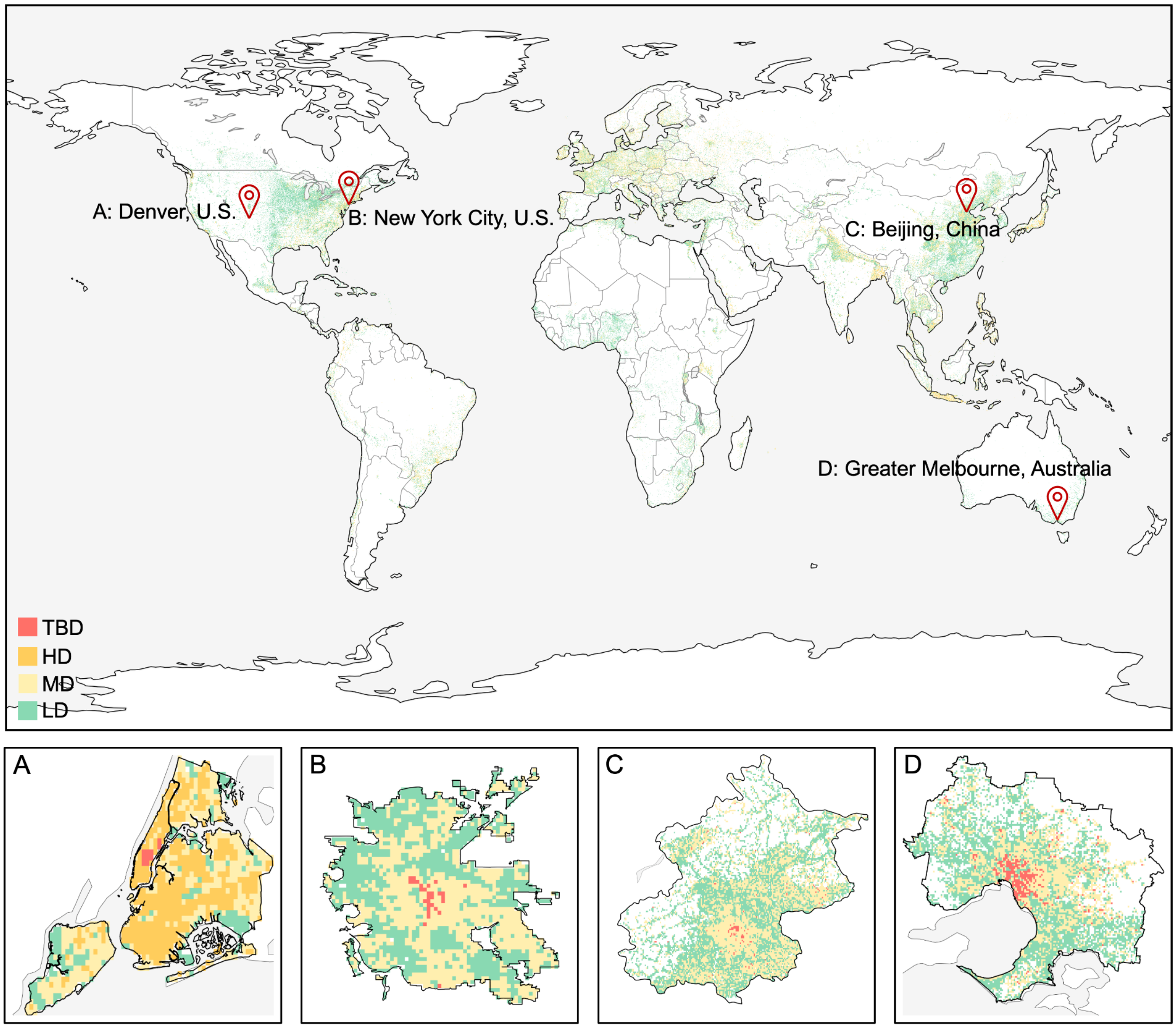

Figure S2. Classification of U-Surf into four density classes: TBD (red), HD (orange), MD (yellow), LD (green) based on the canyon height-to-width ratio percentiles from J2010 for the purpose of assigning thermal parameters as described in section 2.2.3 of the main text. The lower plots illustrate this classification in four selected cities: (A) Denver, U.S., (B) New York City, U.S., (C) Beijing, China, (D) Greater Melbourne, Australia.

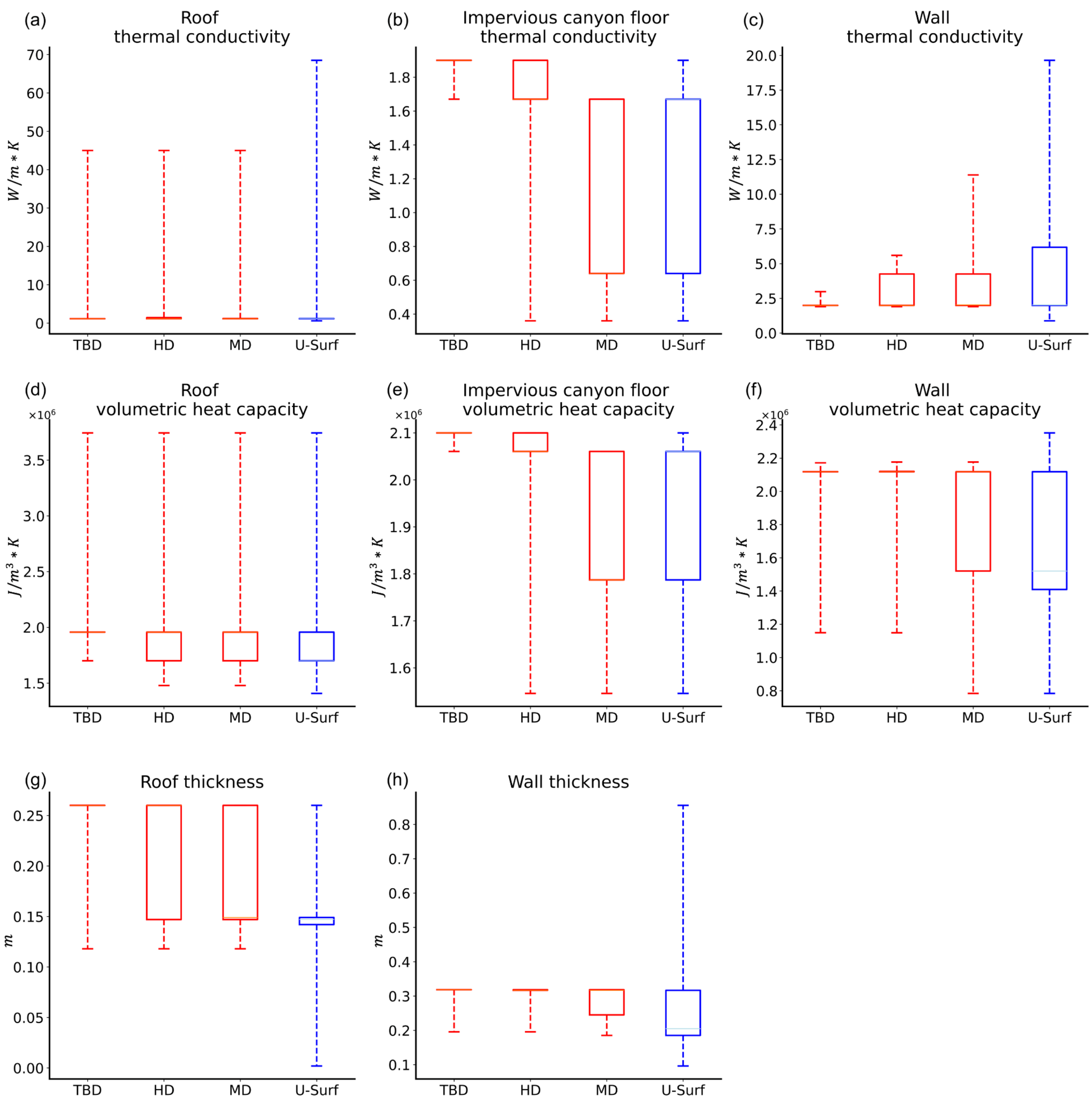

Figure S3. Distributions of thermal properties. Red bars represent default CLMU values (discrete, 33 regions, 3 density classes), and blue bars show the raw new U-Surf values (continuous, 1km). Values of thermal properties are derived based on Oleson and Feddema, (2020).

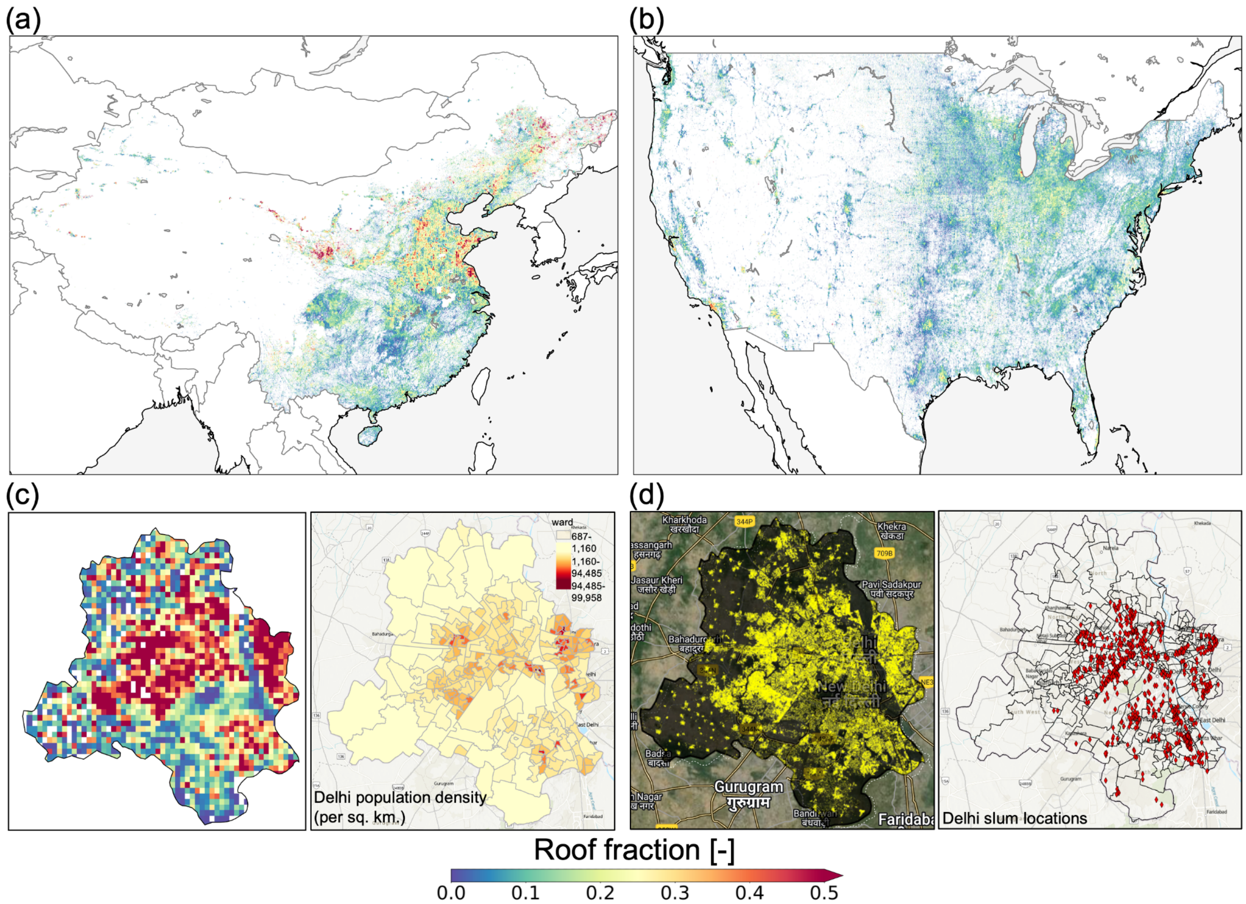

Figure S4. Roof fraction at 1 km-resolution in: (a) China, (b) CONUS, (c) Delhi, India – roof fraction (left) and population density (2022) (right; data source: Esri India, 2024). (d) Delhi, India—building footprints used to derive roof fraction (left) and slum locations (2011) (right; data source: OpenCity - Urban Data Portal, 2024; Delhi Public Geoportal, 2024). All roof fraction maps share the same color scale.

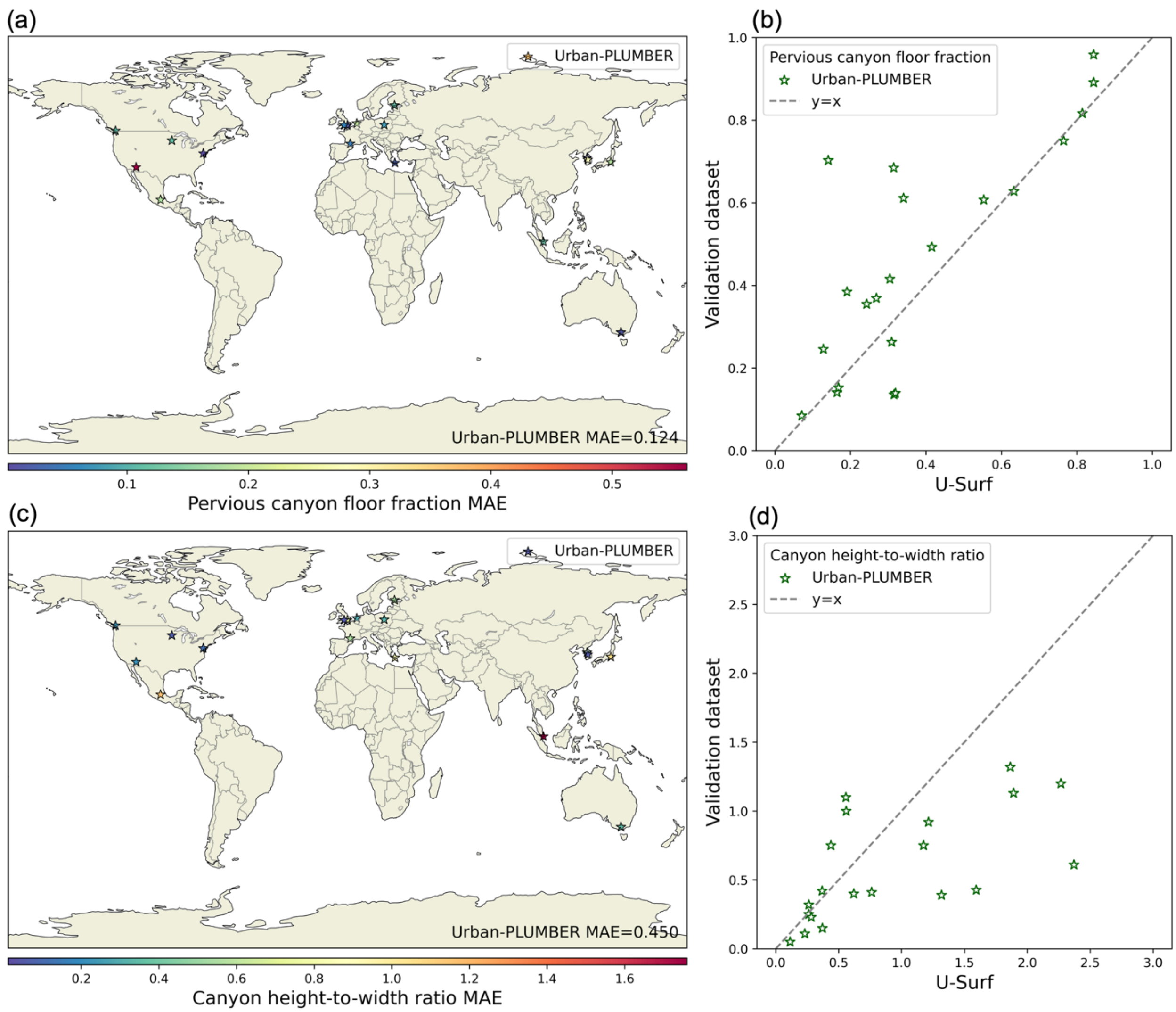

Figure S5. Comparison of two morphological parameters: (a-b) pervious canyon floor fraction, (c-d) canyon height-to-width ratio, against 21 Urban-PLUMBER sites. The numbers labeled on the bottom right corner of (a) and (c) represent the average mean absolute error across sites.

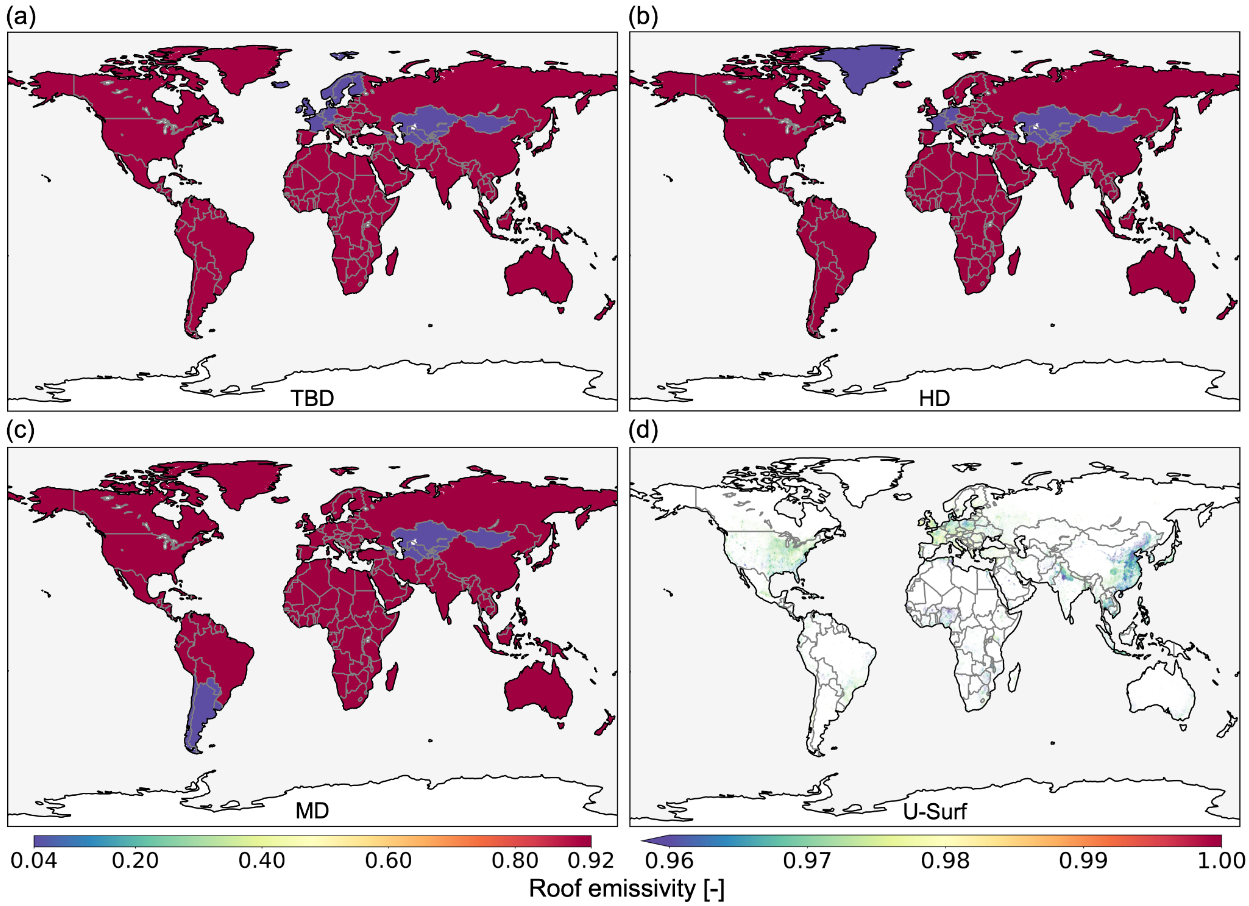

Figure S6. Comparison between CLMU, including (a) Tall Building District (TBD), (b) High Density (HD), (c) Medium Density (MD) (categorical values), and (d) U-Surf roof emissivity (1km resolution) at global scale. Note that (a-c) CLMU parameters share a common colorbar at the bottom left and (d) U-Surf parameter uses a separate one (bottom right) for visualization purposes.

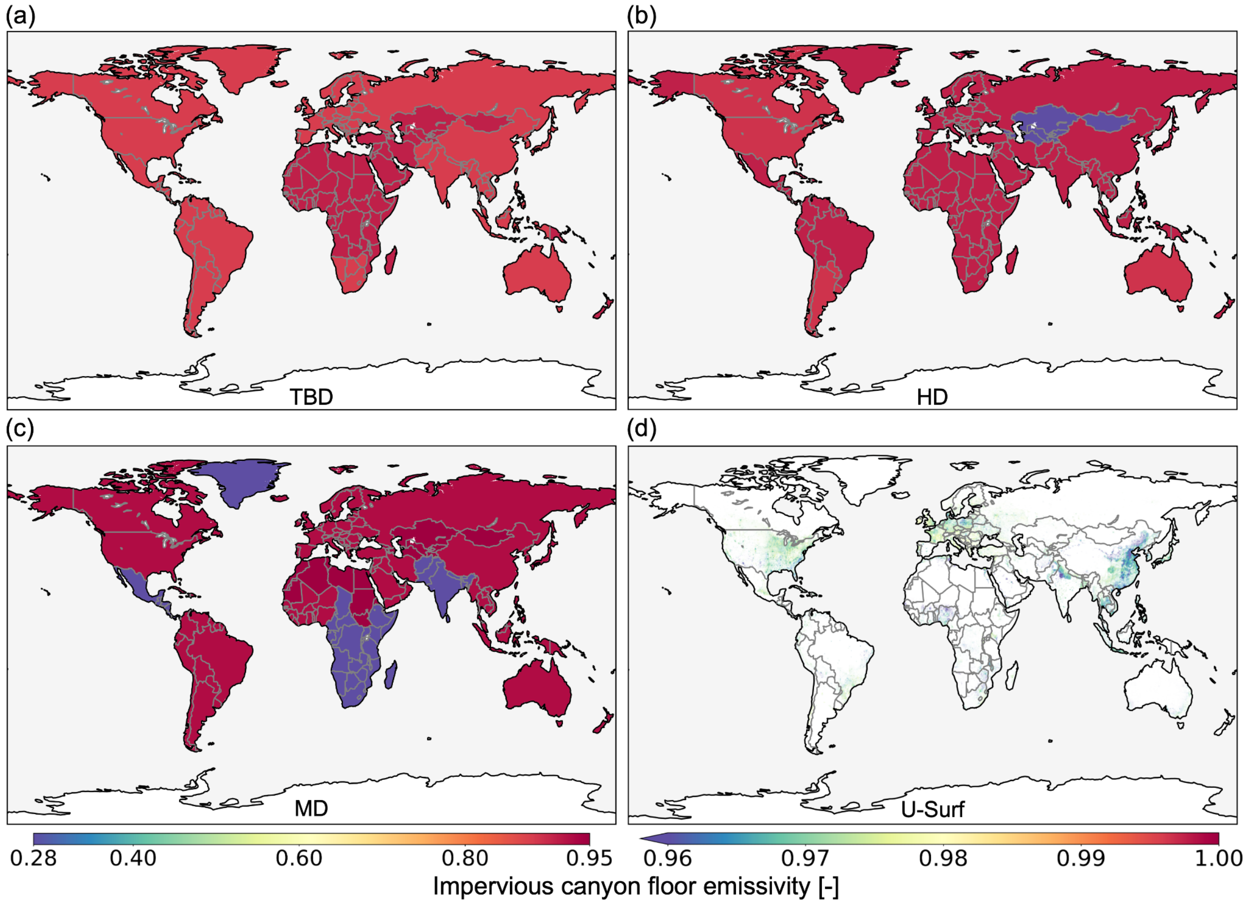

Figure S7. Same as S6, but for impervious canyon floor emissivity.

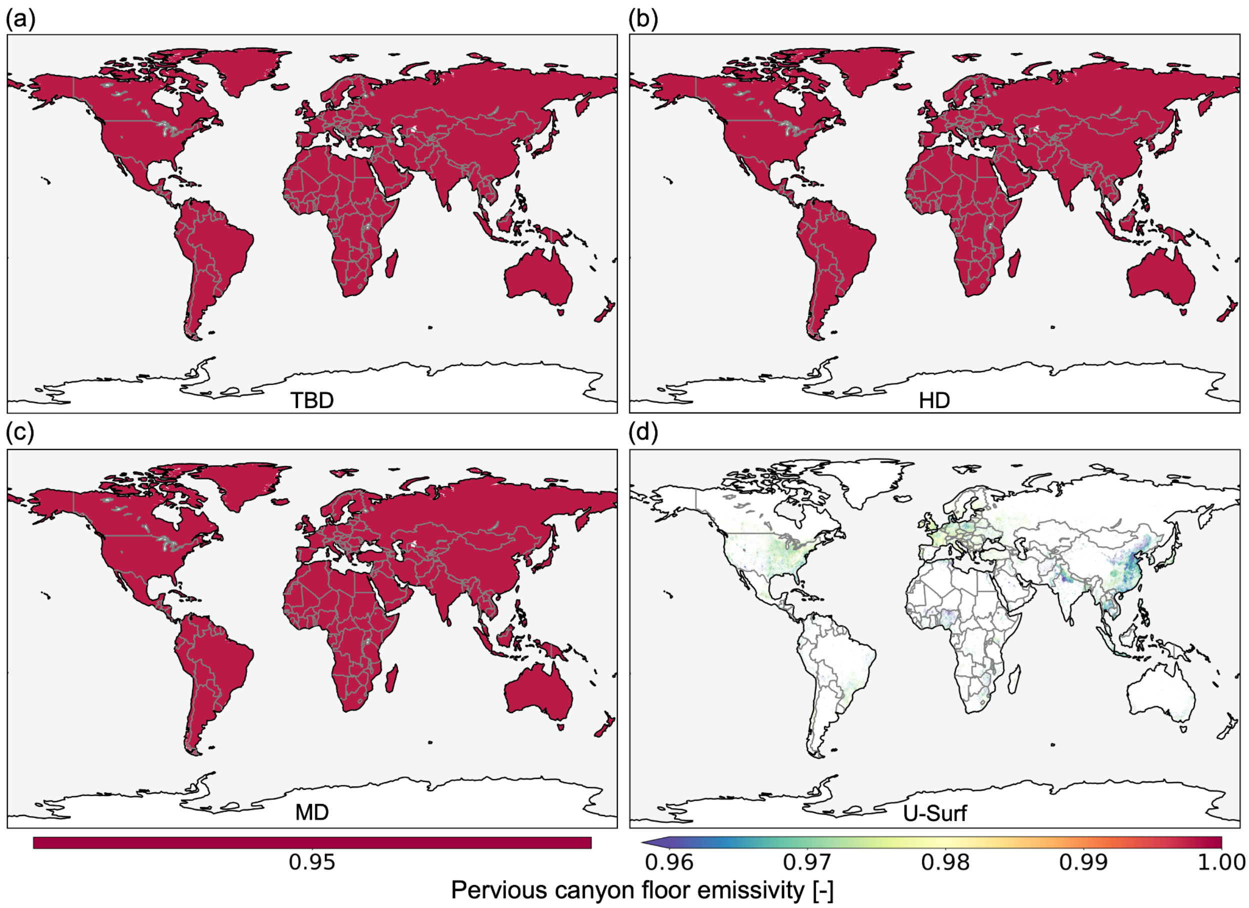

Figure S8. Same as S6, but for pervious canyon floor emissivity. Note that the emissivity is set to be 0.95 everywhere to represent a typical value for vegetation using a bulk parameterization scheme (Oleson et al., 2010).

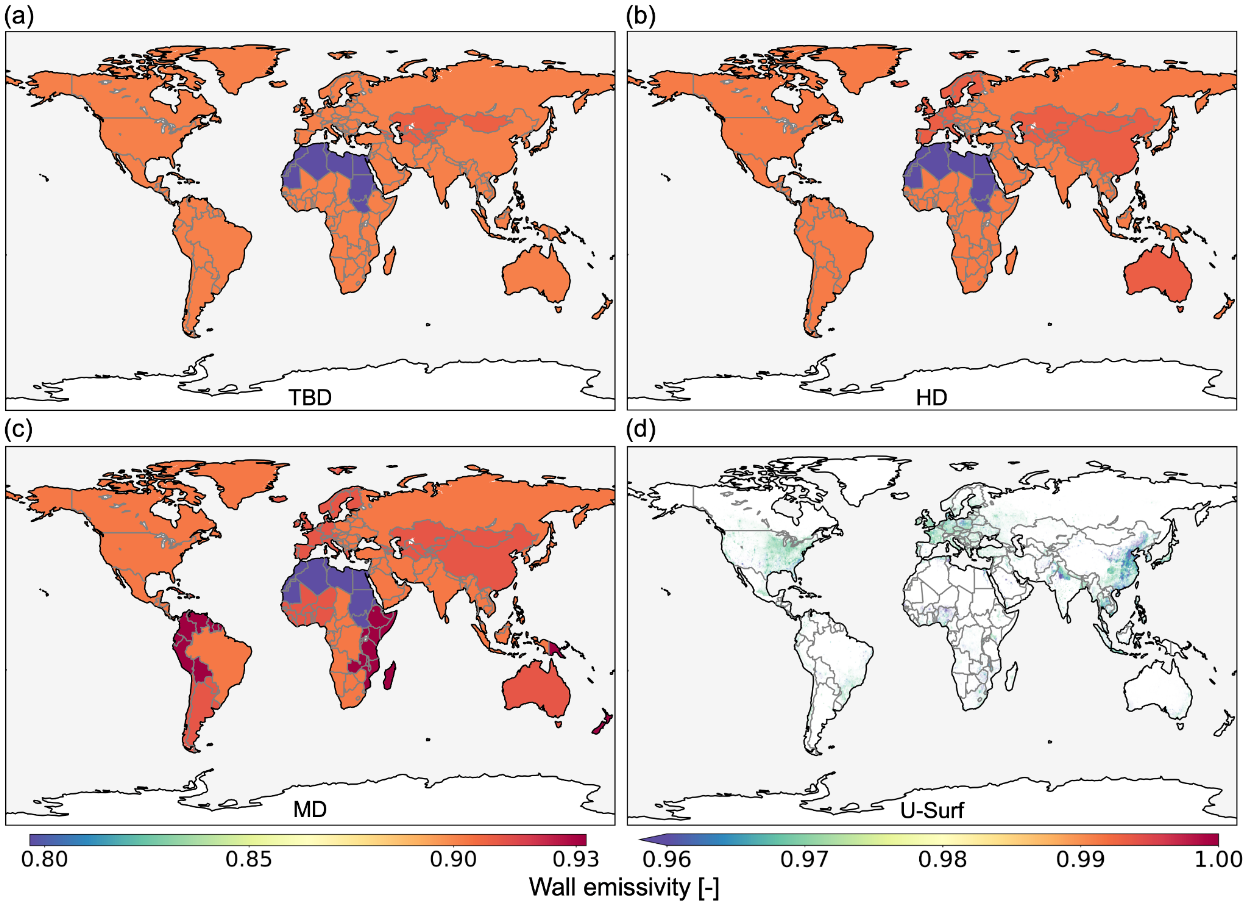

Figure S9. Same as S6, but for wall emissivity.

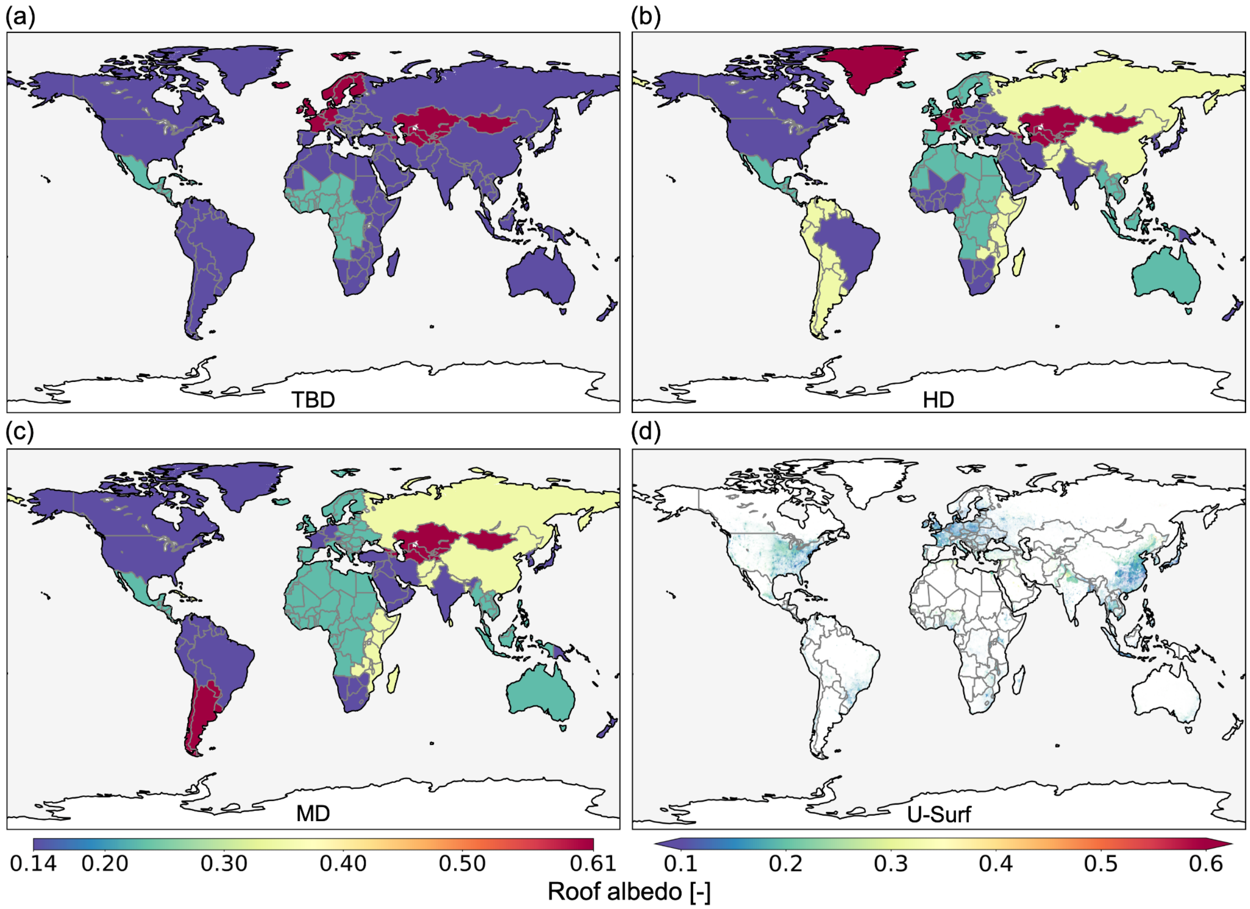

Figure S10. Same as S6, but for roof albedo.

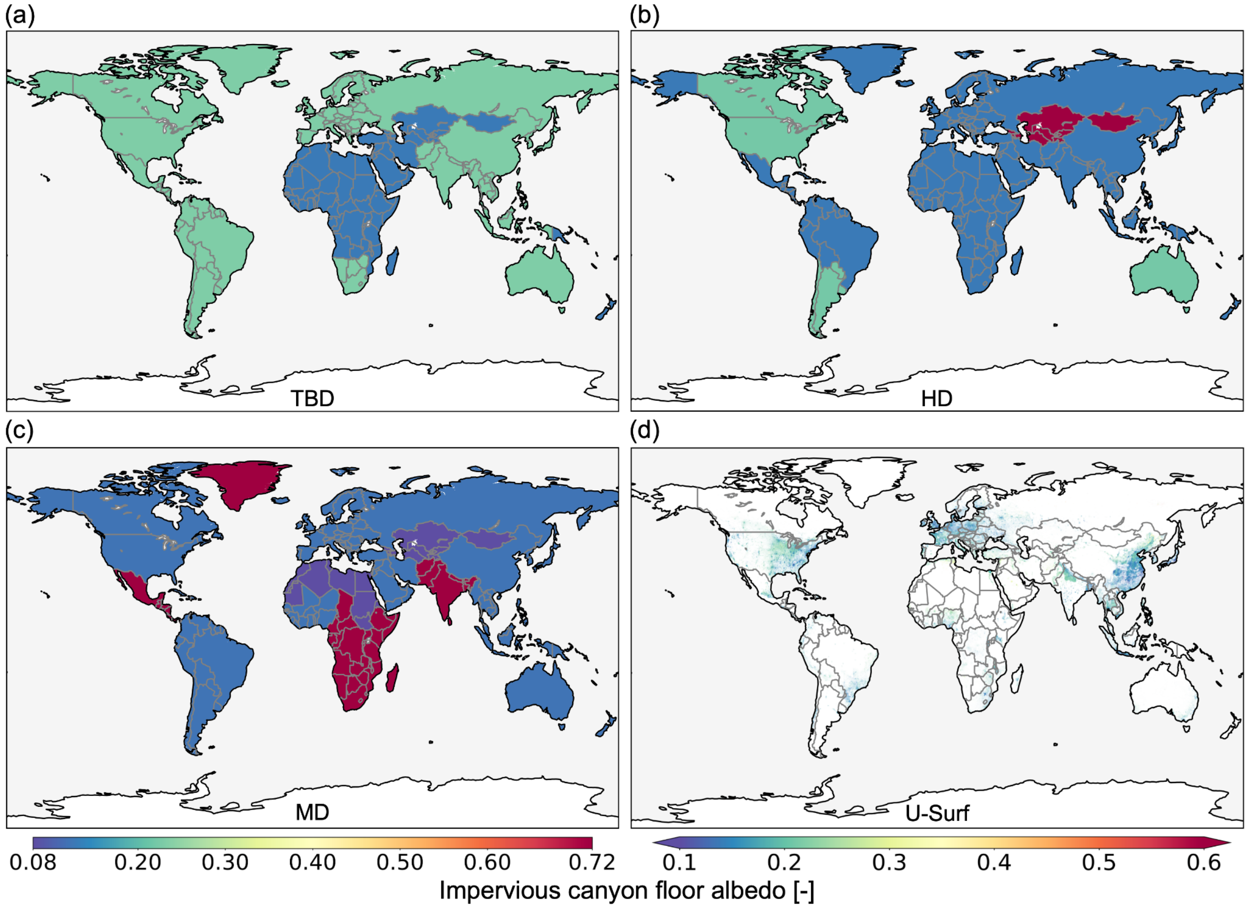

Figure S11. Same as S6, but for impervious canyon floor albedo.

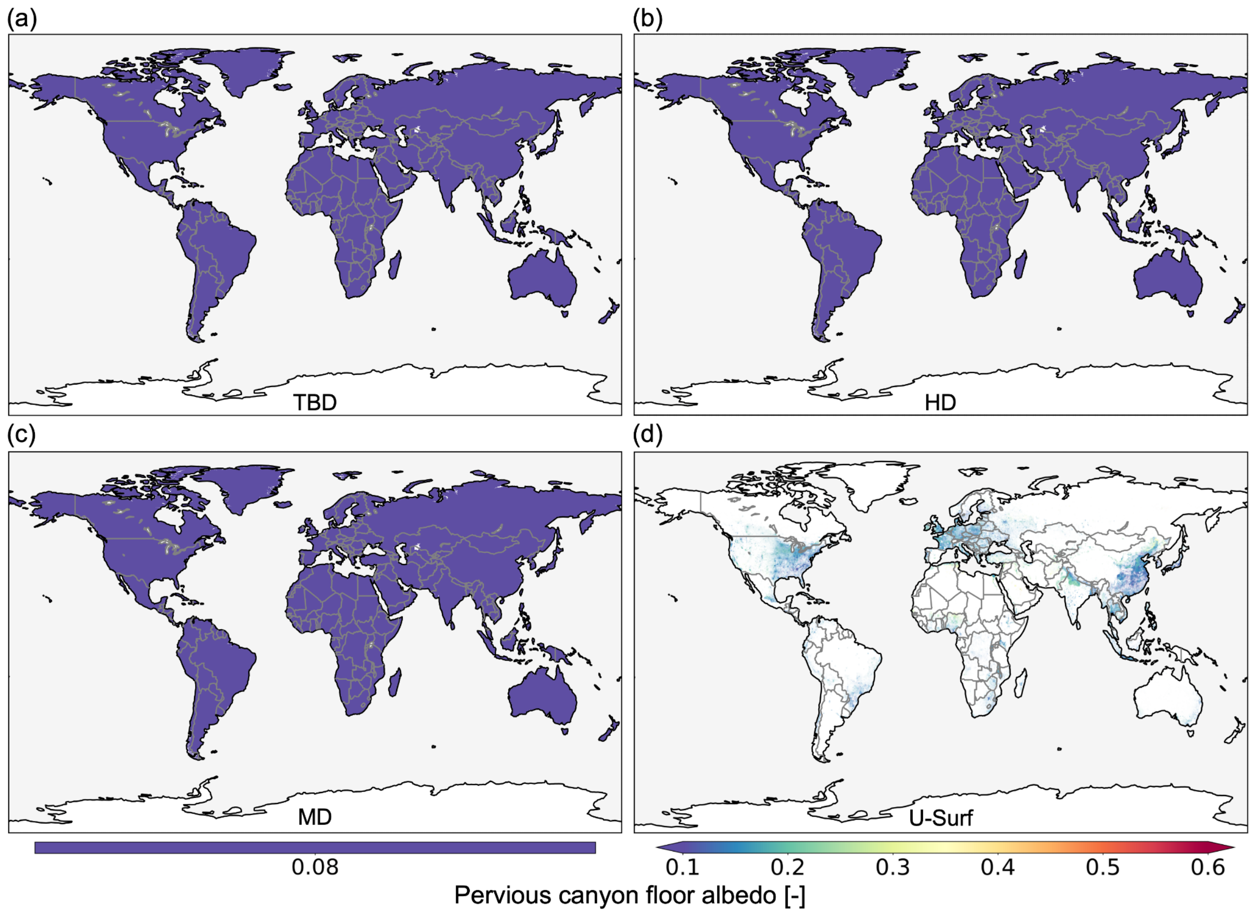

Figure S12. Same as S6, but for pervious canyon floor albedo. Note that the albedo is set to be 0.08 everywhere to represent a typical value for vegetation using a bulk parameterization scheme (Oleson et al., 2010).

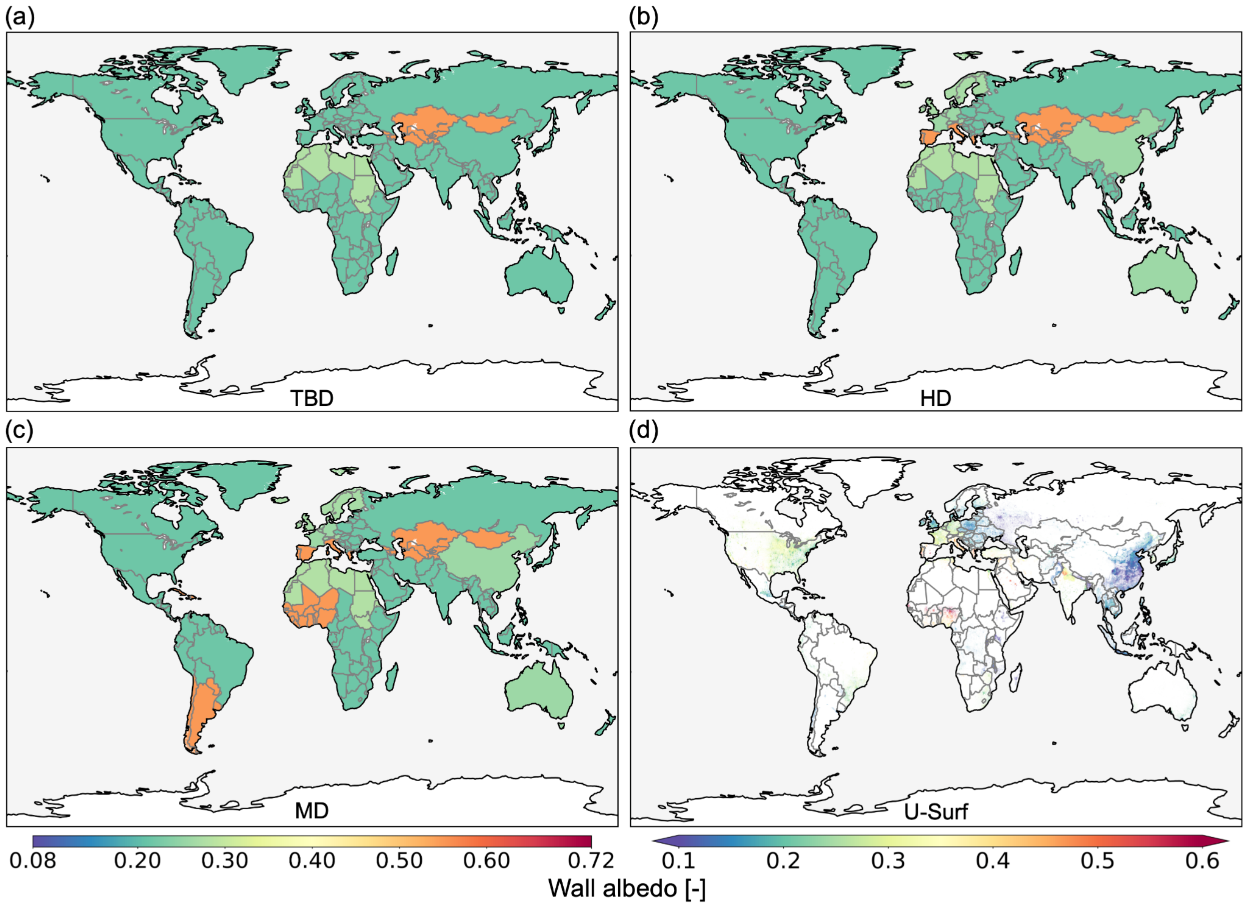

Figure S13. Same as S6, but for wall albedo.

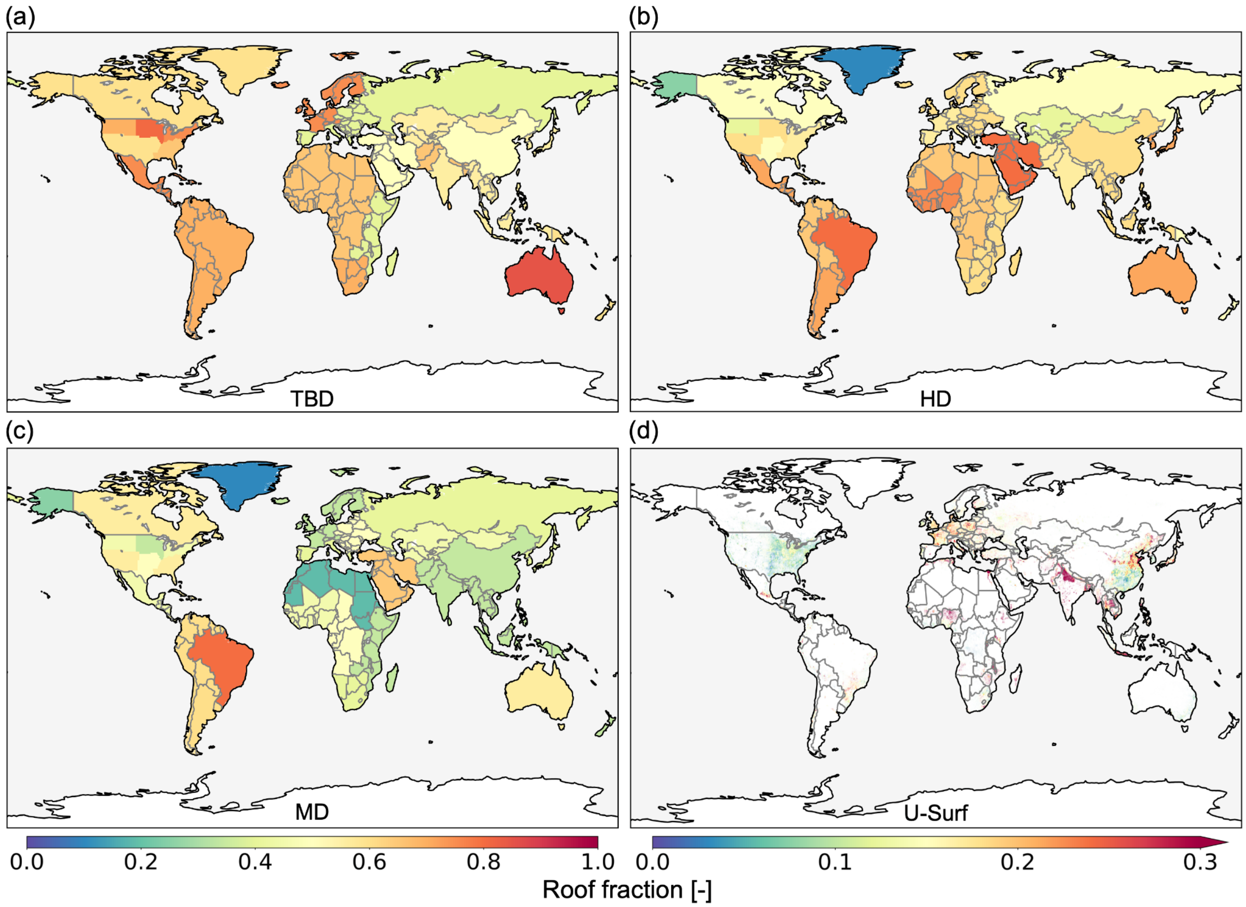

Figure S14. Same as S6, but for roof fraction.

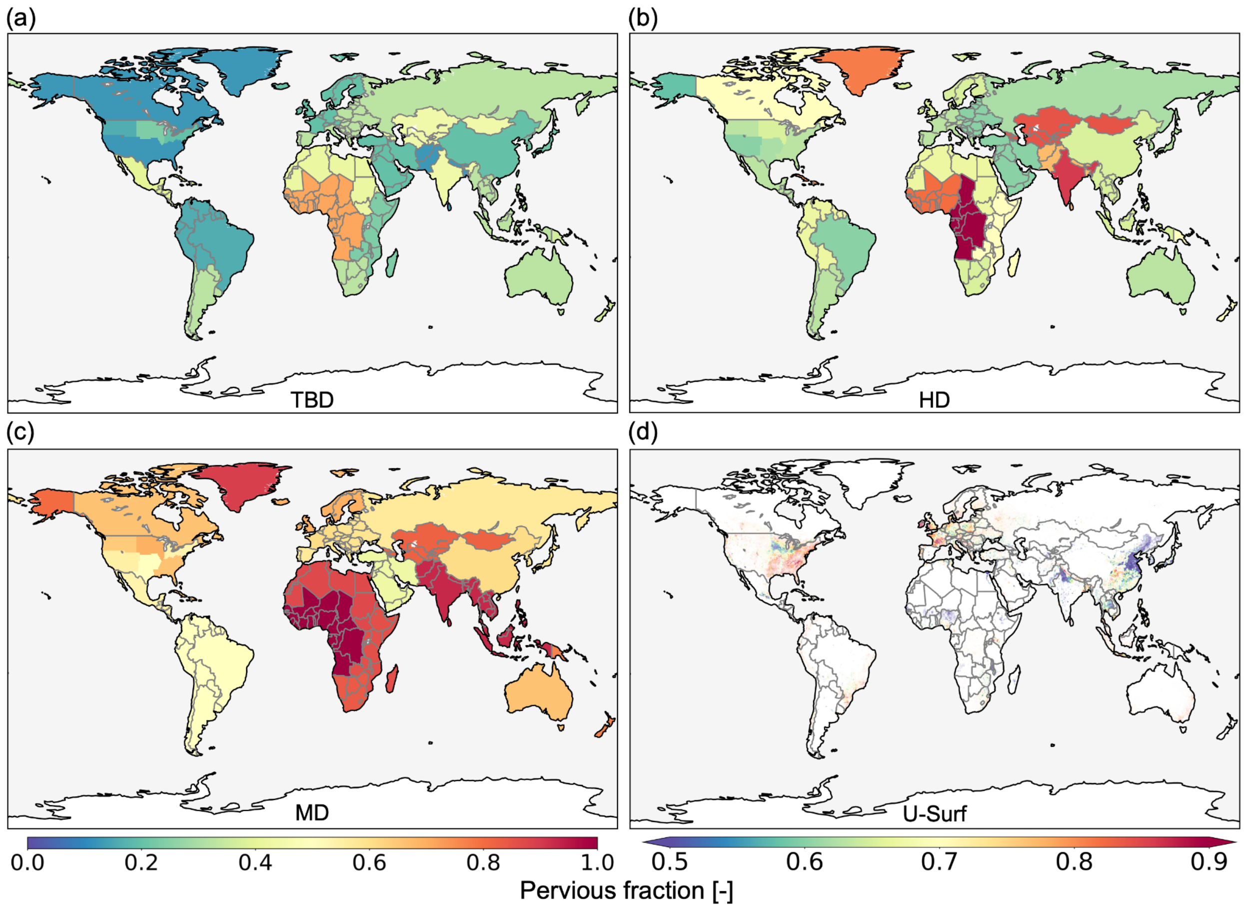

Figure S15. Same as S6, but for pervious fraction of the canyon floor.

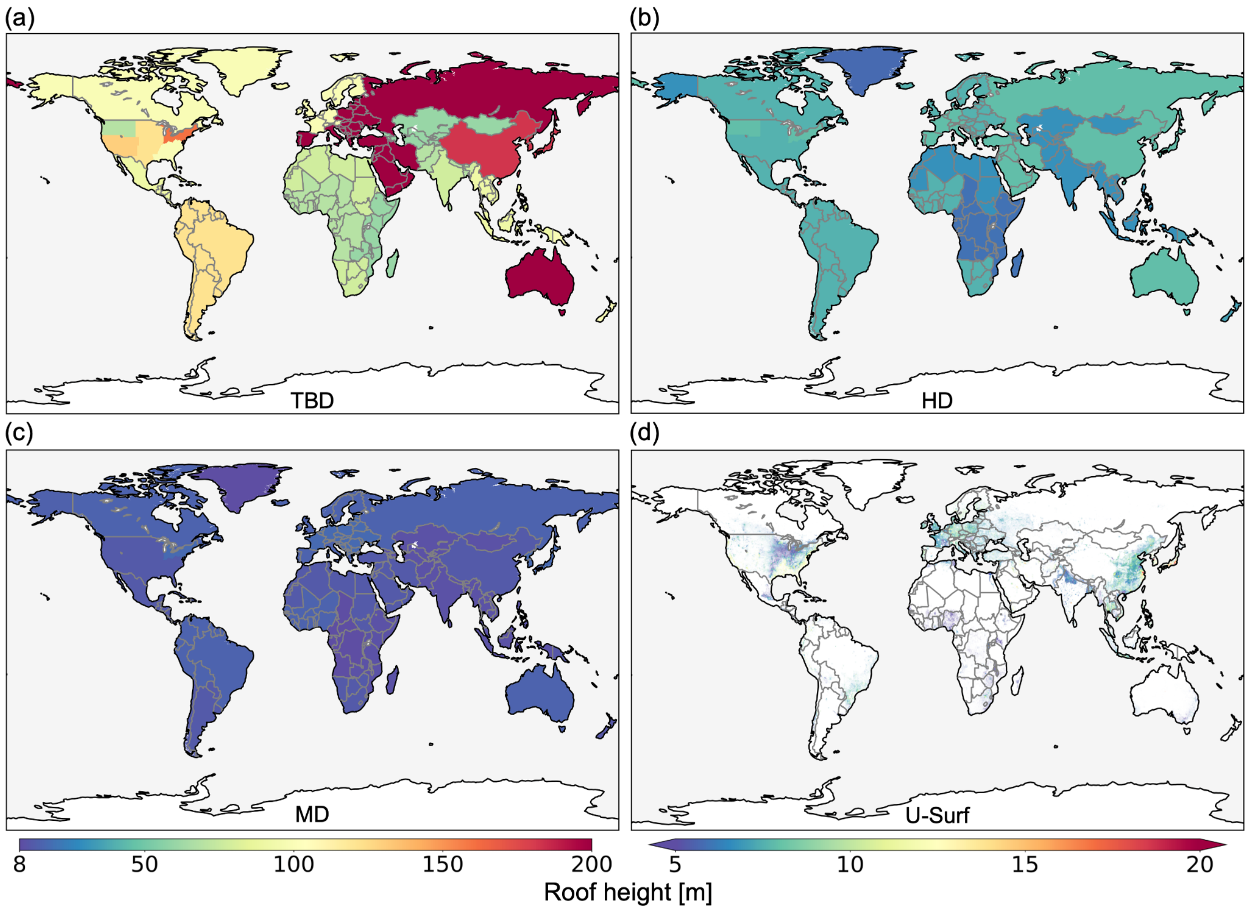

Figure S16. Same as S6, but for roof height [meter].

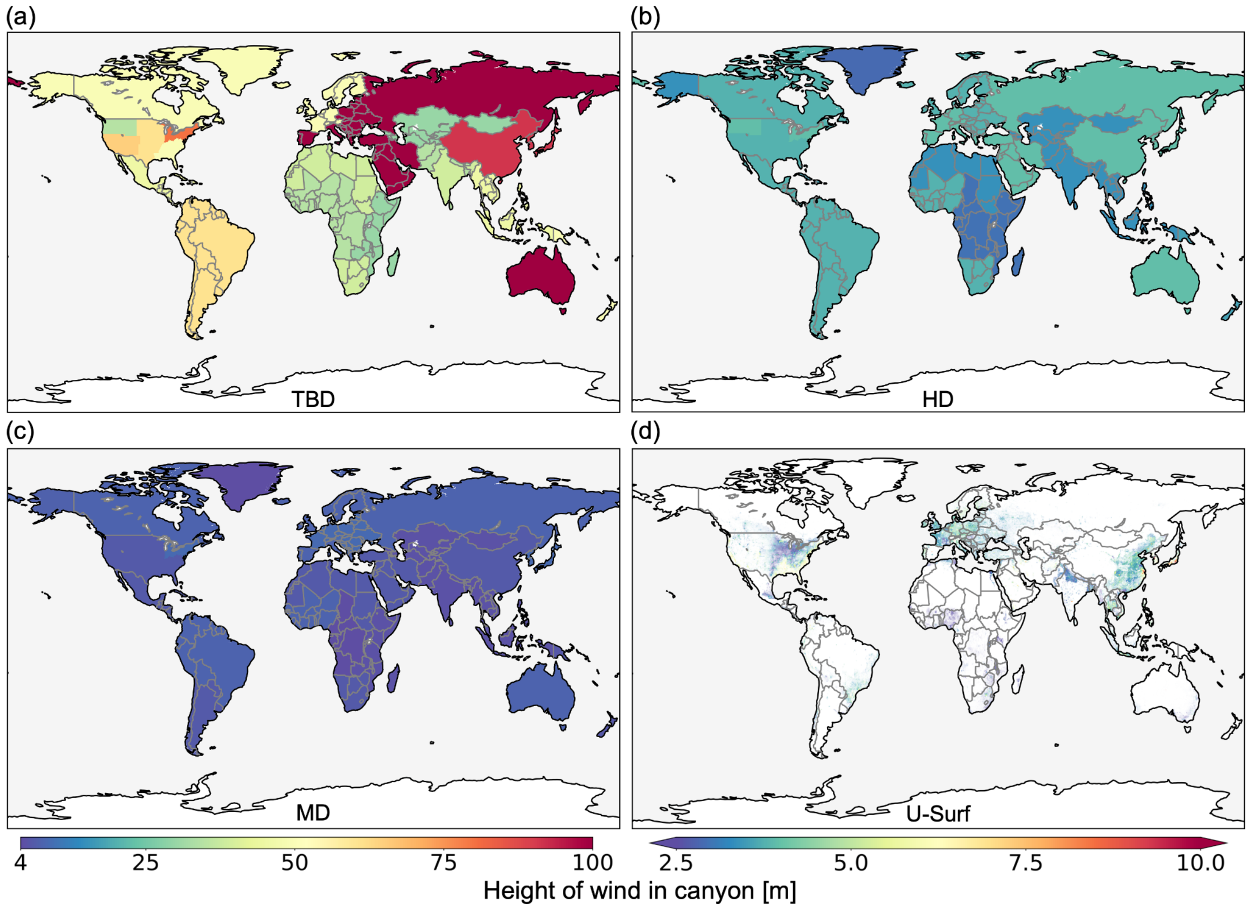

Figure S17. Same as S6, but for height of wind in canyon [meter].

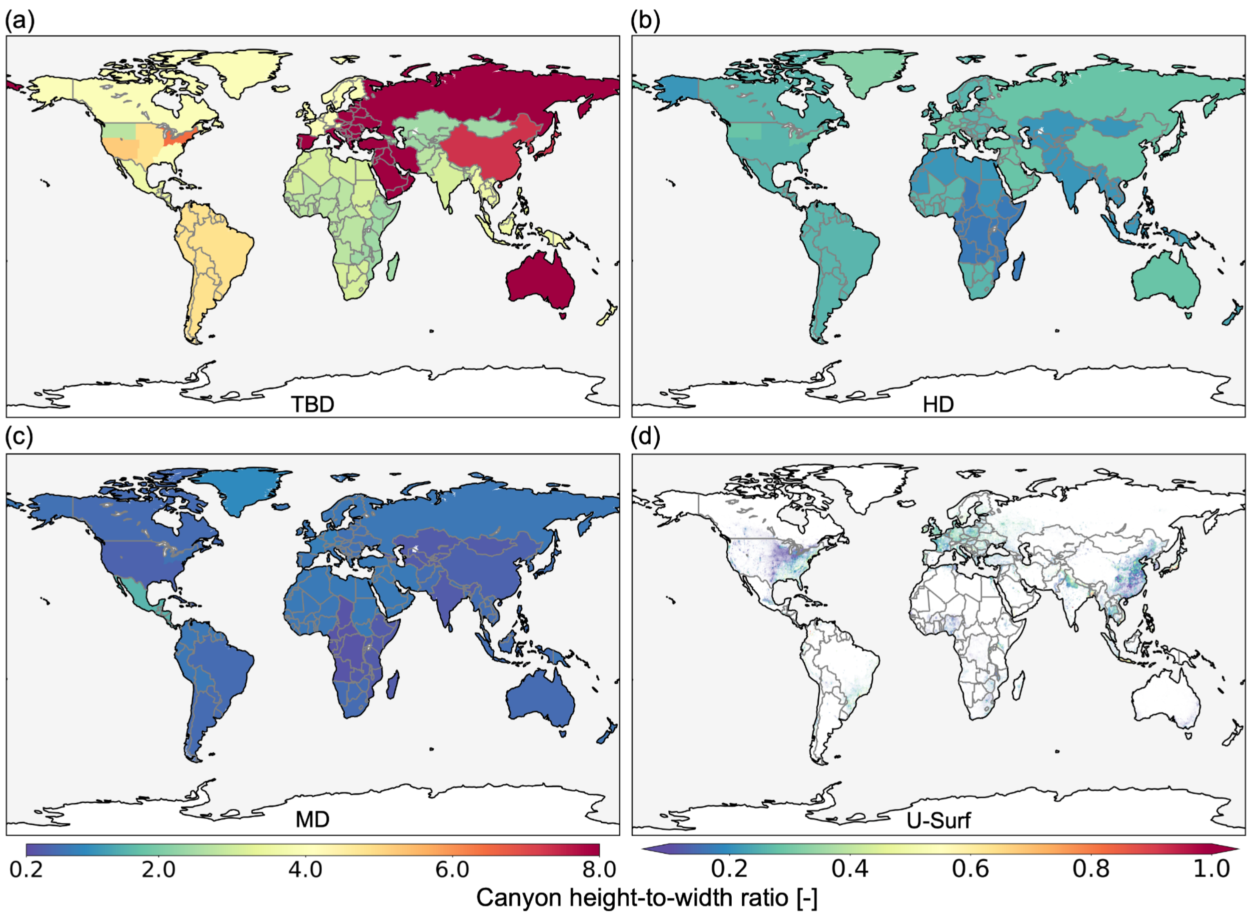

Figure S18. Same as S6, but for canyon height-to-width ratio.

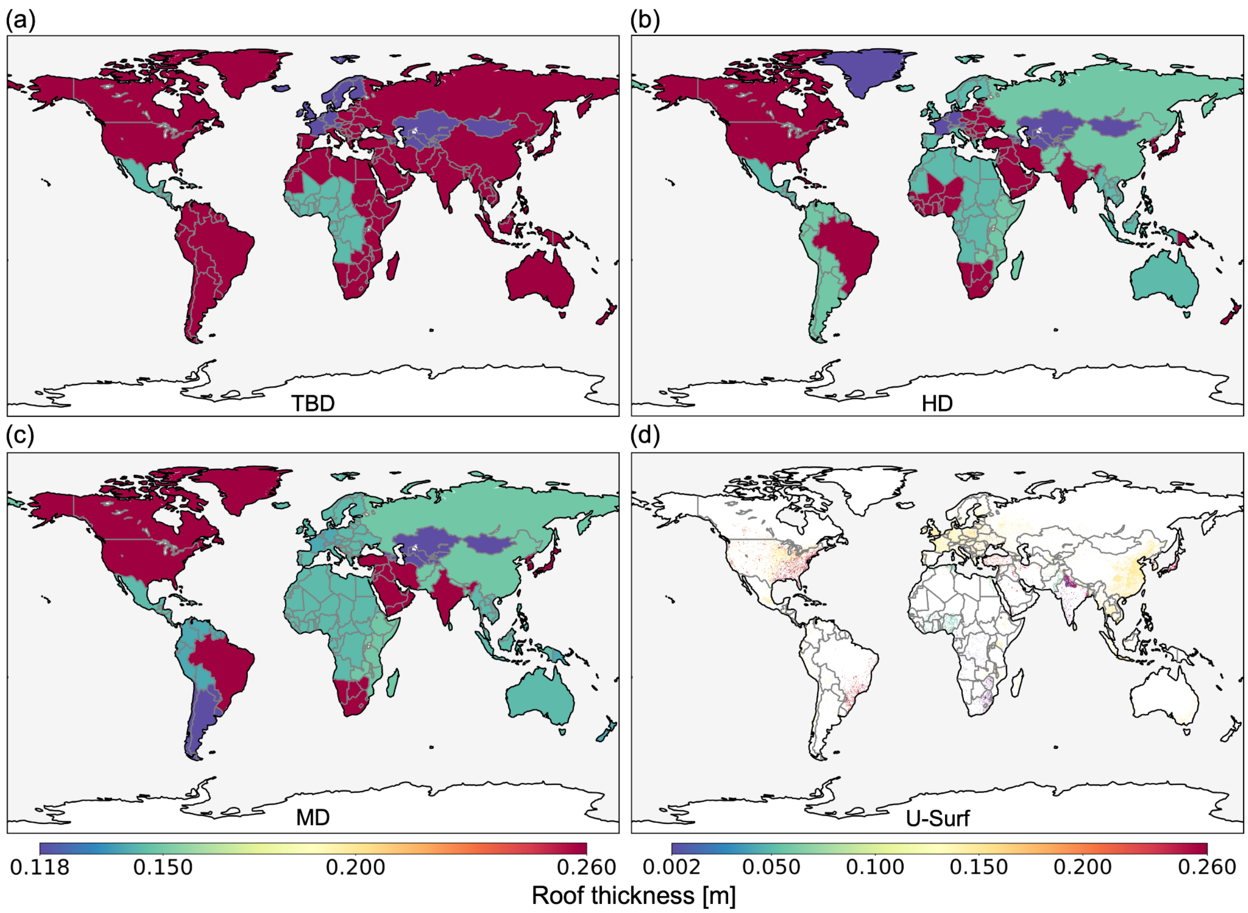

Figure S19. Same as S6, but for roof thickness [meter].

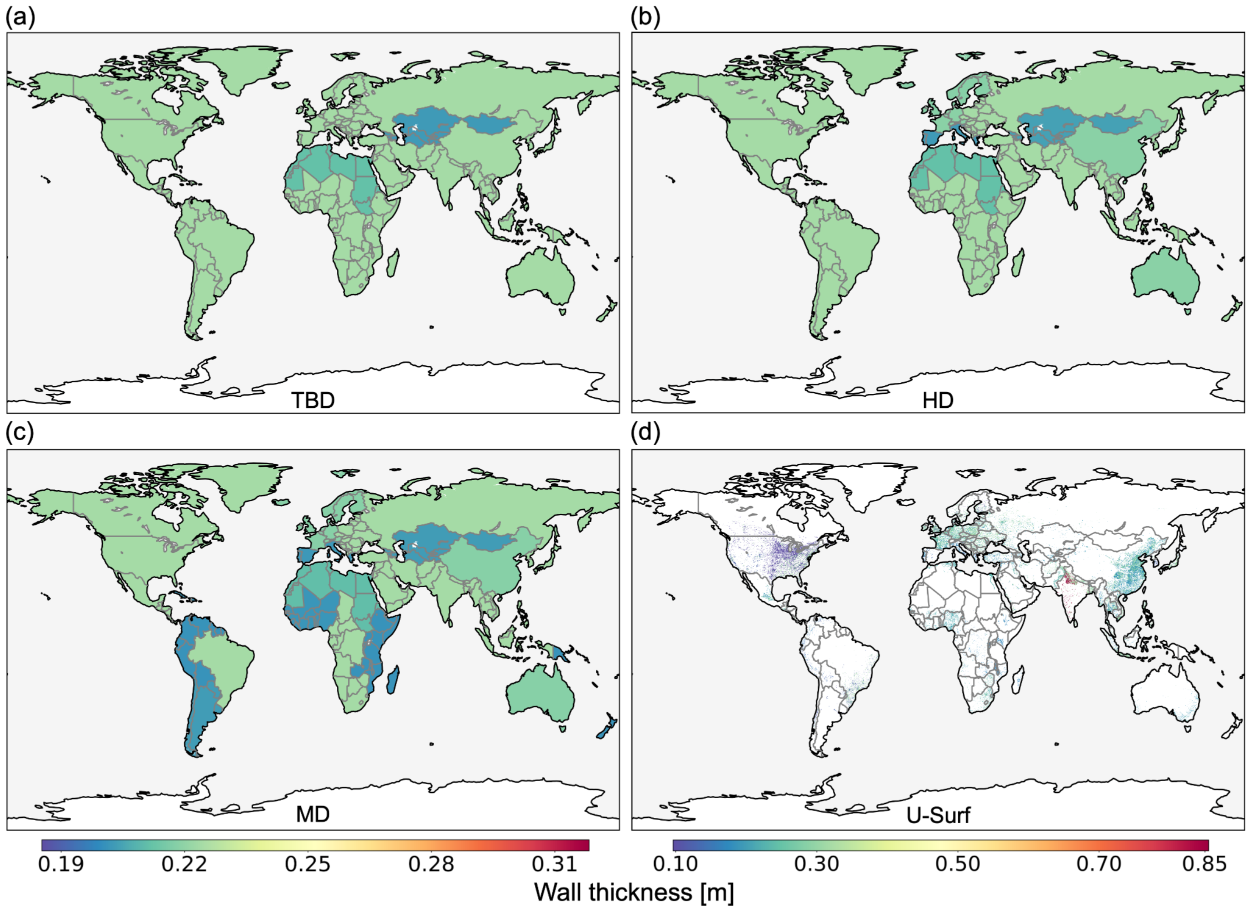

Figure S20. Same as S19, but for wall thickness [meter].

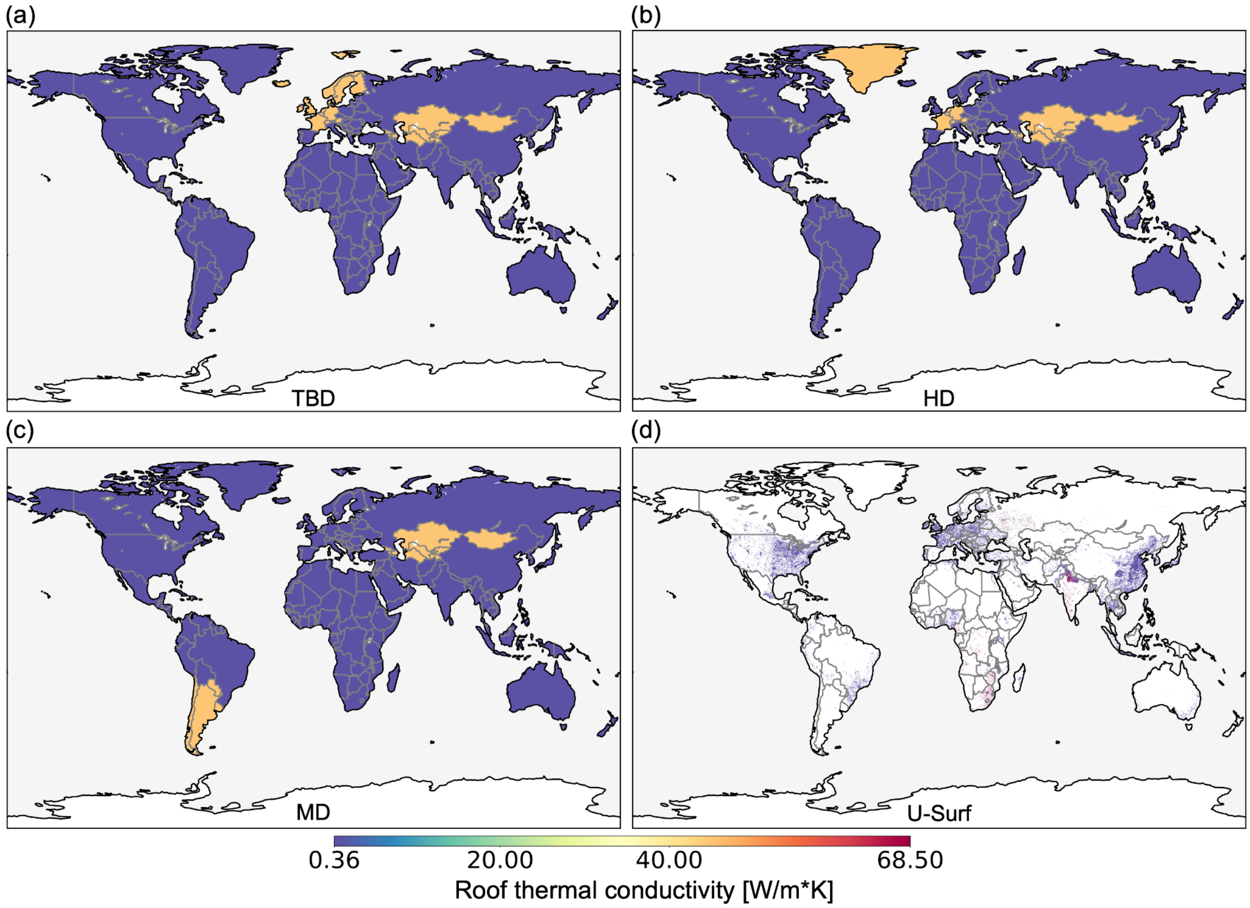

Figure S21. Same as S19, but for roof thermal conductivity $[W/m \cdot K]$. Note that there are 10 distinct layers for roofs and walls, each comes with a different value for thermal conductivity and volumetric heat capacity that depends on the material of each layer. The maps only show the value of the first layer for visualization purposes.

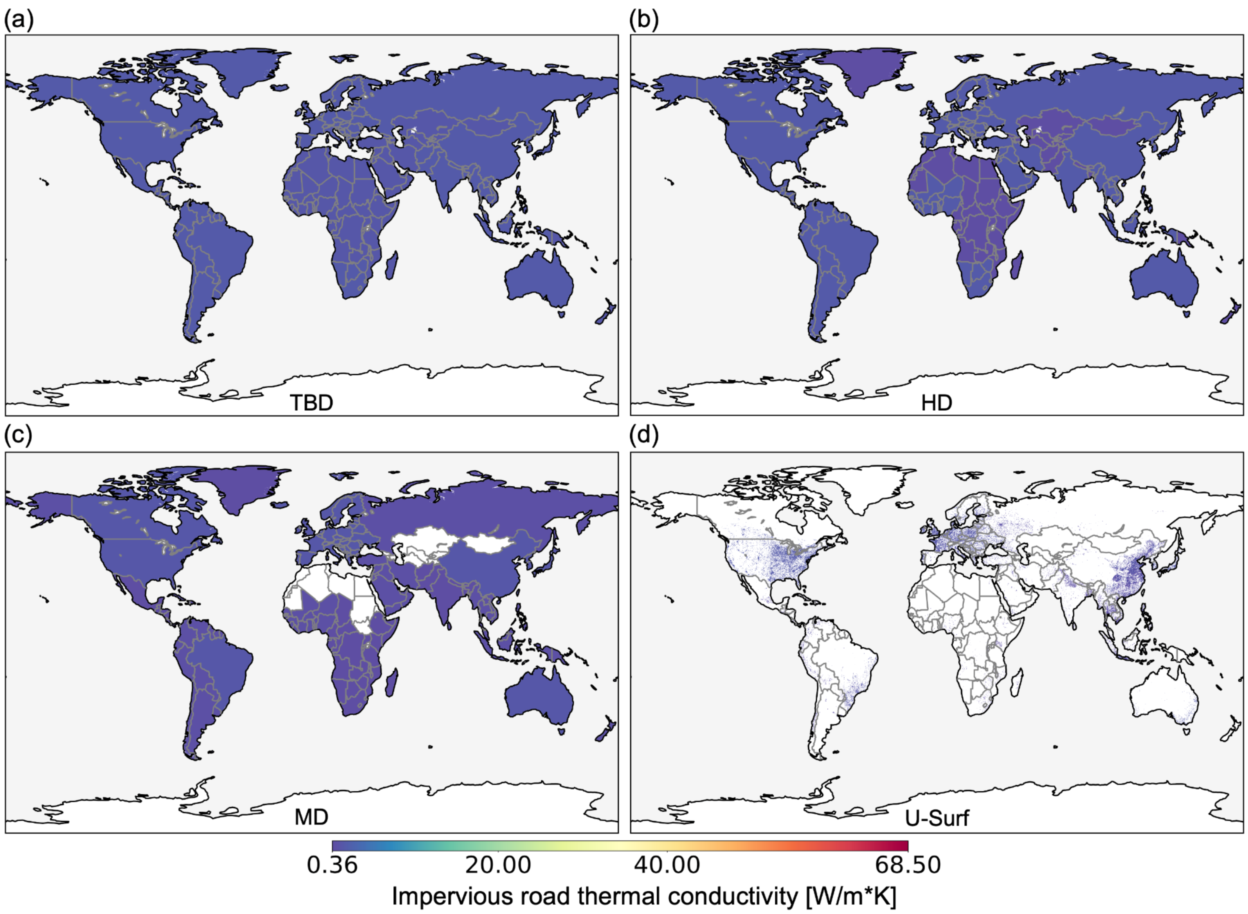

Figure S22. Same as S21, but for impervious canyon floor thermal conductivity $[W/m \cdot K]$.

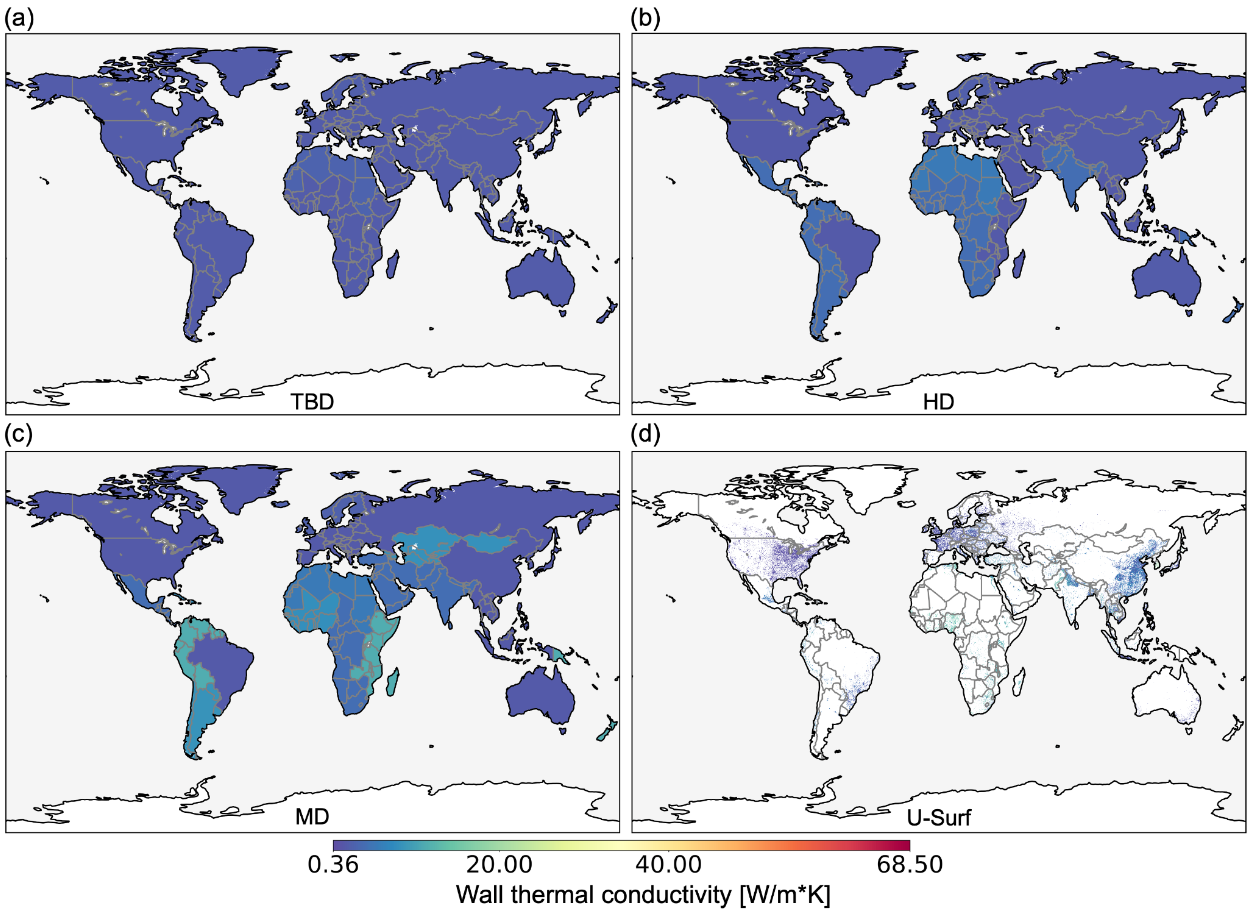

Figure S23. Same as S21, but for wall thermal conductivity $[W/m \cdot K]$.

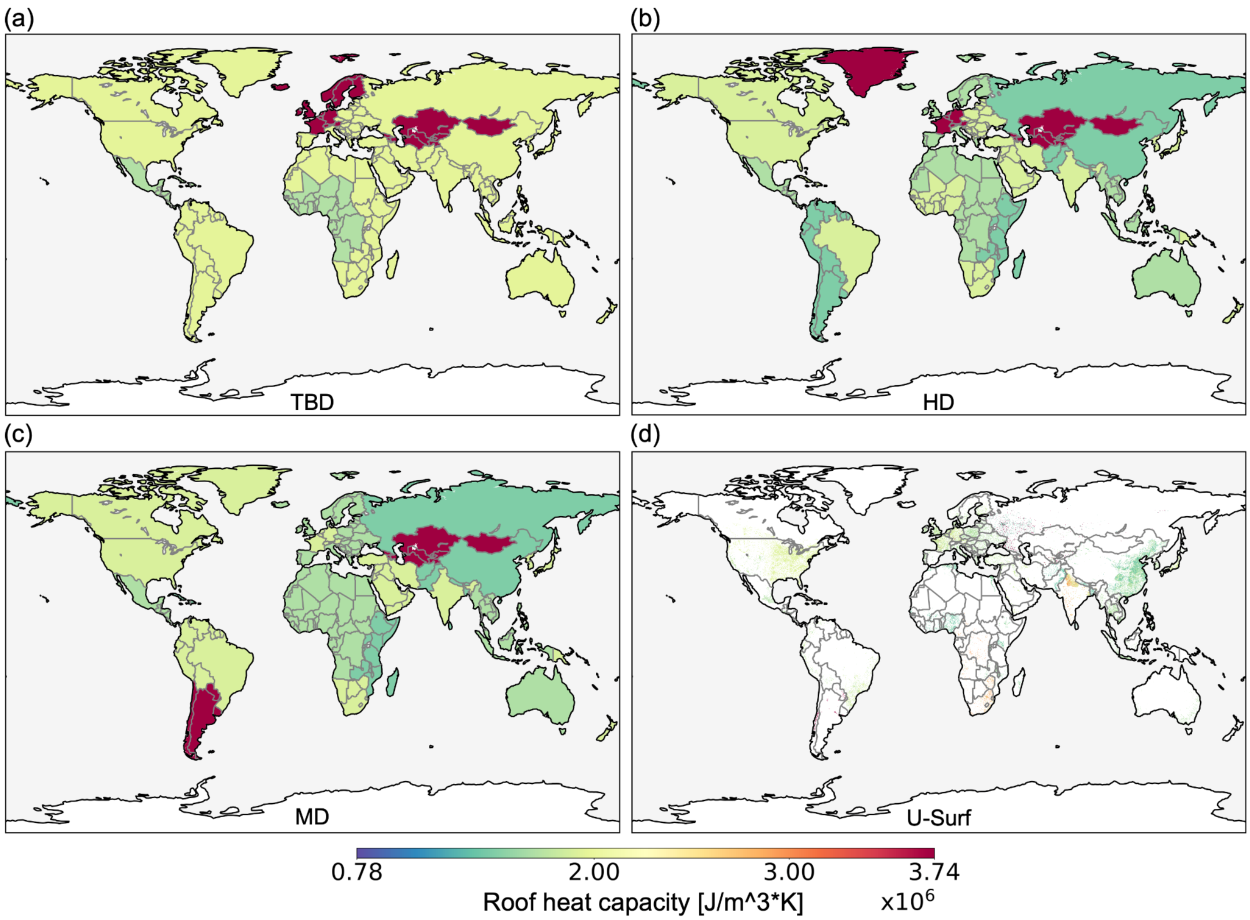

Figure S24. Same as S21, but for roof volumetric heat capacity $[J/m^3 \cdot K]$.

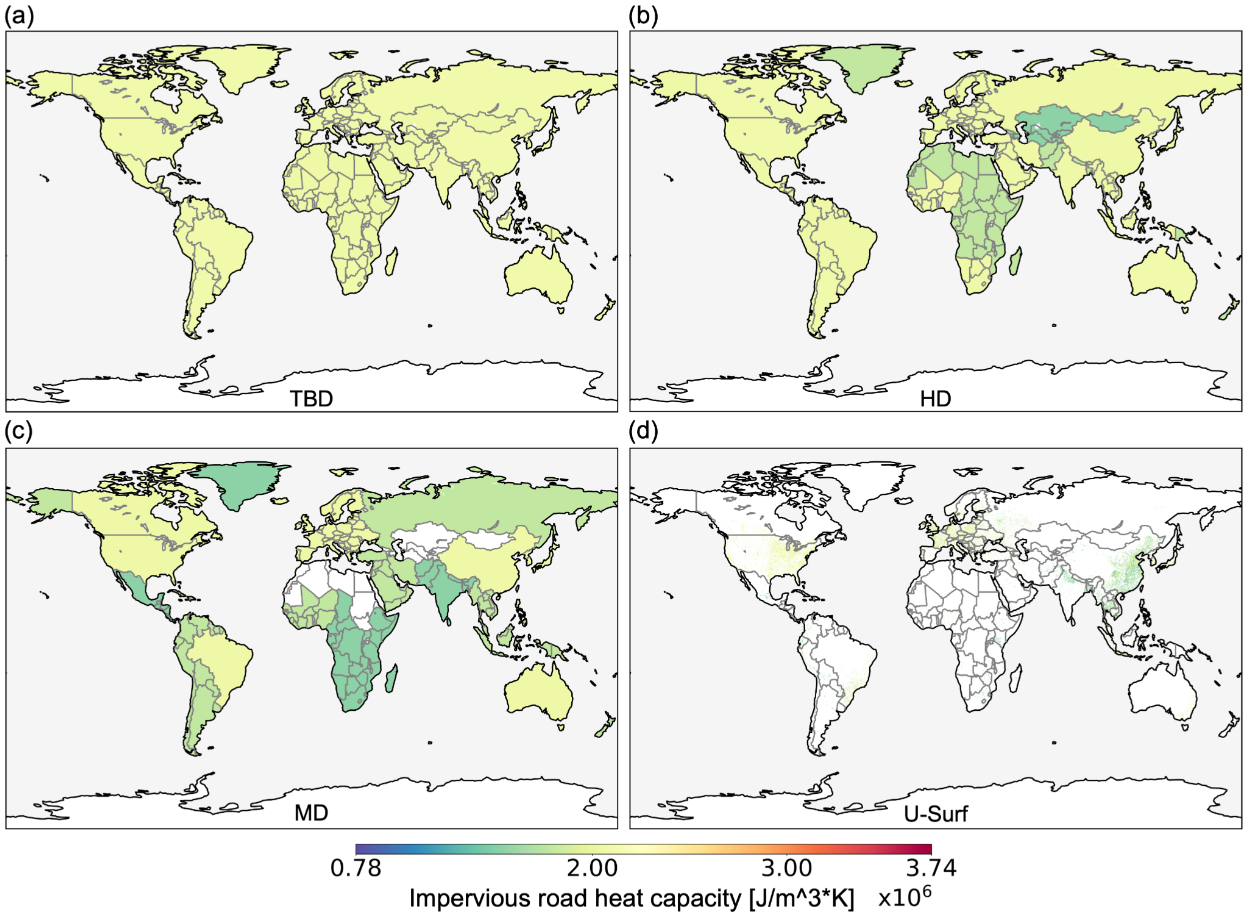

Figure S25. Same as S21, but for impervious volumetric heat capacity $[J/m^3 \cdot K]$.

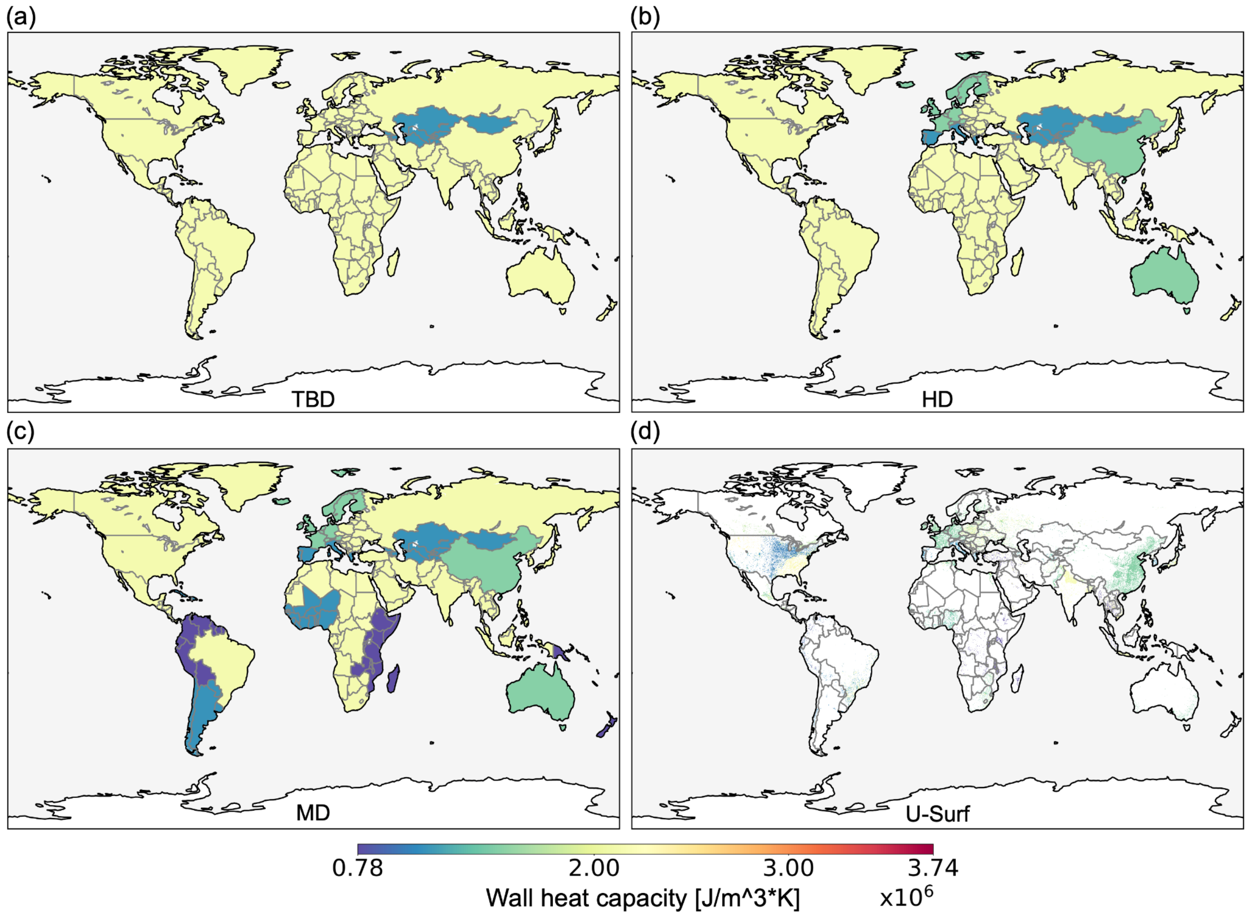

Figure S26. Same as S21, but for wall volumetric heat capacity $[J/m^3 \cdot K]$.

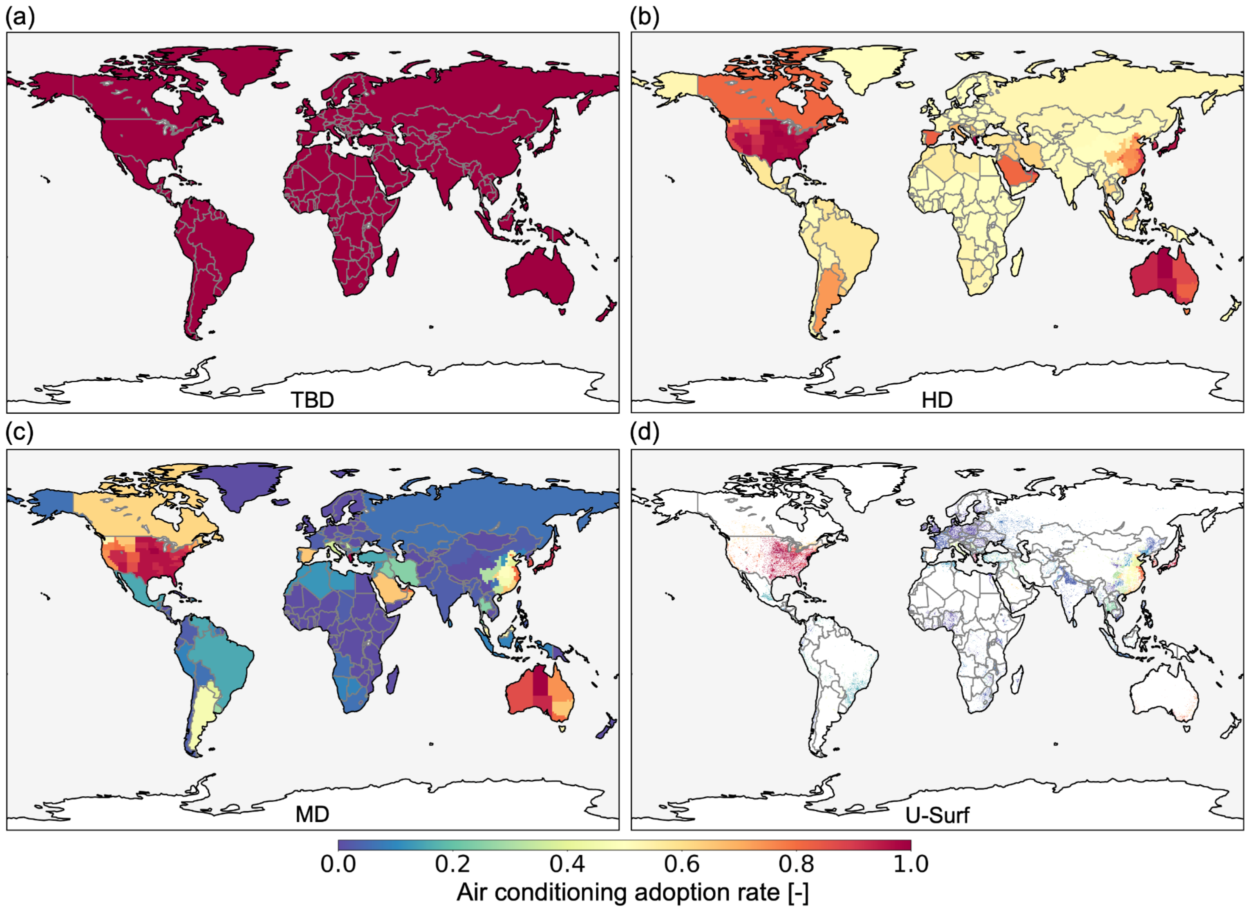

Figure S27. AC adoption rate adapted from Li et al., (2024). Note that the AC adoption rate was collected at national and sub-national level, the gridded dataset used to generate the 1km-resolution map is area-weighted averages of the three density types at 0.9375° × 1.25° (latitude × longitude).

References

Delhi Public Geoportal: https://gsdl.org.in/DelhiPublic.html, last access: 16 September 2024.

Esri India: https://www.esri.in/en-in/home, last access: 16 September 2024.

OpenCity - Urban Data Portal: https://opencity.in/, last access: 16 September 2024.

Jackson, T. L., Feddema, J. J., Oleson, K. W., Bonan, G. B., and Bauer, J. T.: Parameterization of Urban Characteristics for Global Climate Modeling, Annals of the Association of American Geographers, 100, 848–865, https://doi.org/10.1080/00045608.2010.497328, 2010.

Li, X. "Cathy," Zhao, L., Oleson, K., Zhou, Y., Qin, Y., Zhang, K., and Fang, B.: Enhancing Urban Climate-Energy Modeling in the Community Earth System Model (CESM) Through Explicit Representation of Urban Air-Conditioning Adoption, Journal of Advances in Modeling Earth Systems, 16, e2023MS004107, https://doi.org/10.1029/2023MS004107, 2024.

Oleson, K., Bonan, B., Feddema, J., Vertenstein, M., and Kluzek, E.: Technical Description of an Urban Parameterization for the Community Land Model (CLMU), https://doi.org/10.5065/D6K35RM9, 2010.

Oleson, K. W. and Feddema, J.: Parameterization and Surface Data Improvements and New Capabilities for the Community Land Model Urban (CLMU), Journal of Advances in Modeling Earth Systems, 12, e2018MS001586, https://doi.org/10.1029/2018MS001586, 2020.